Supplementary Figure S1

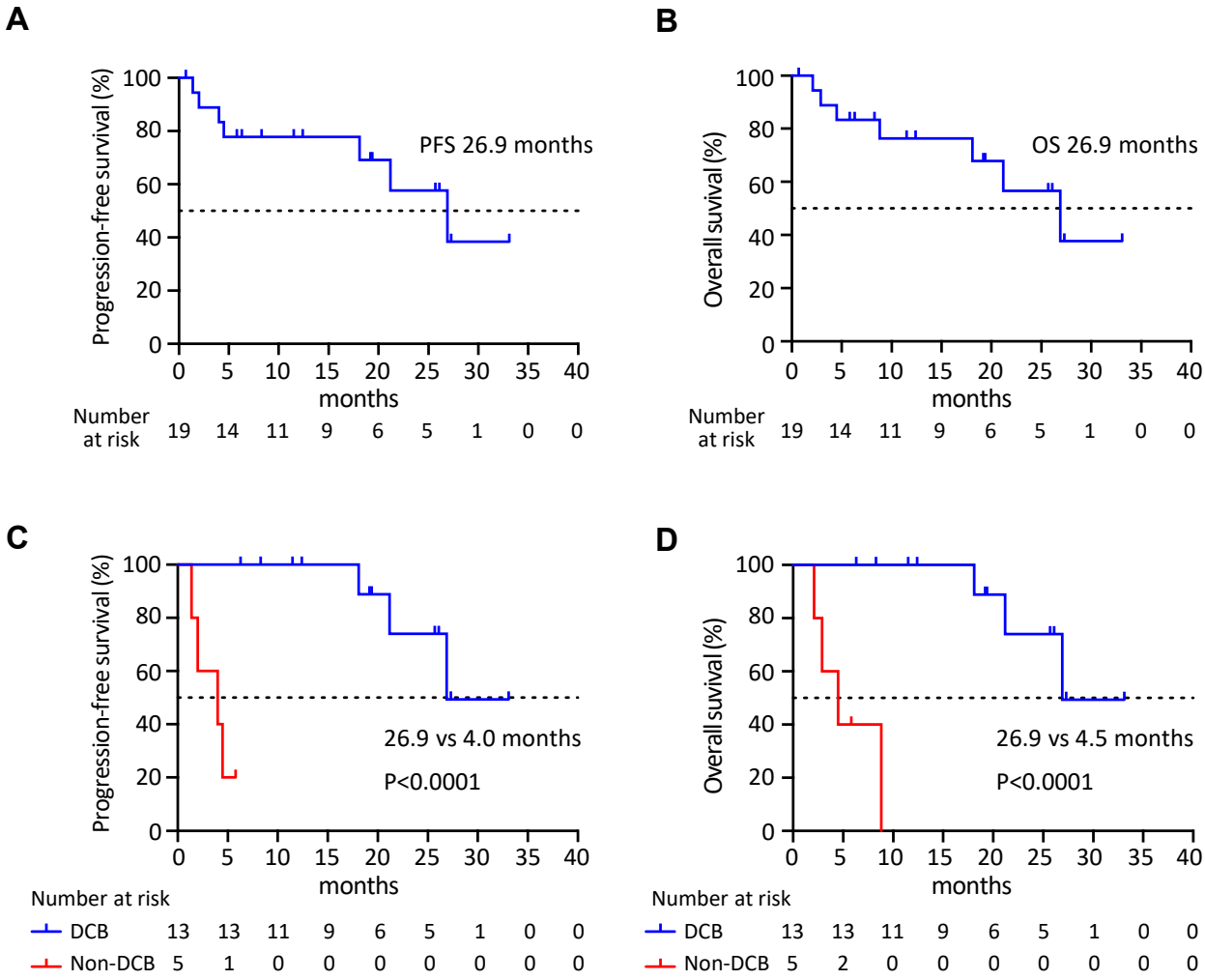

Supplemental figure S1. Survival analysis of microsatellite instability-high (MSI-H) gastric cancer (GC) **A.** progression-free survival in all enrolled patients. **B.** overall survival in all enrolled patients. **C.** progression-free survival between durable clinical benefit (DCB) group and non-DCB group. **D**. overall survival between durable clinical benefit (DCB) group and non-DCB group.

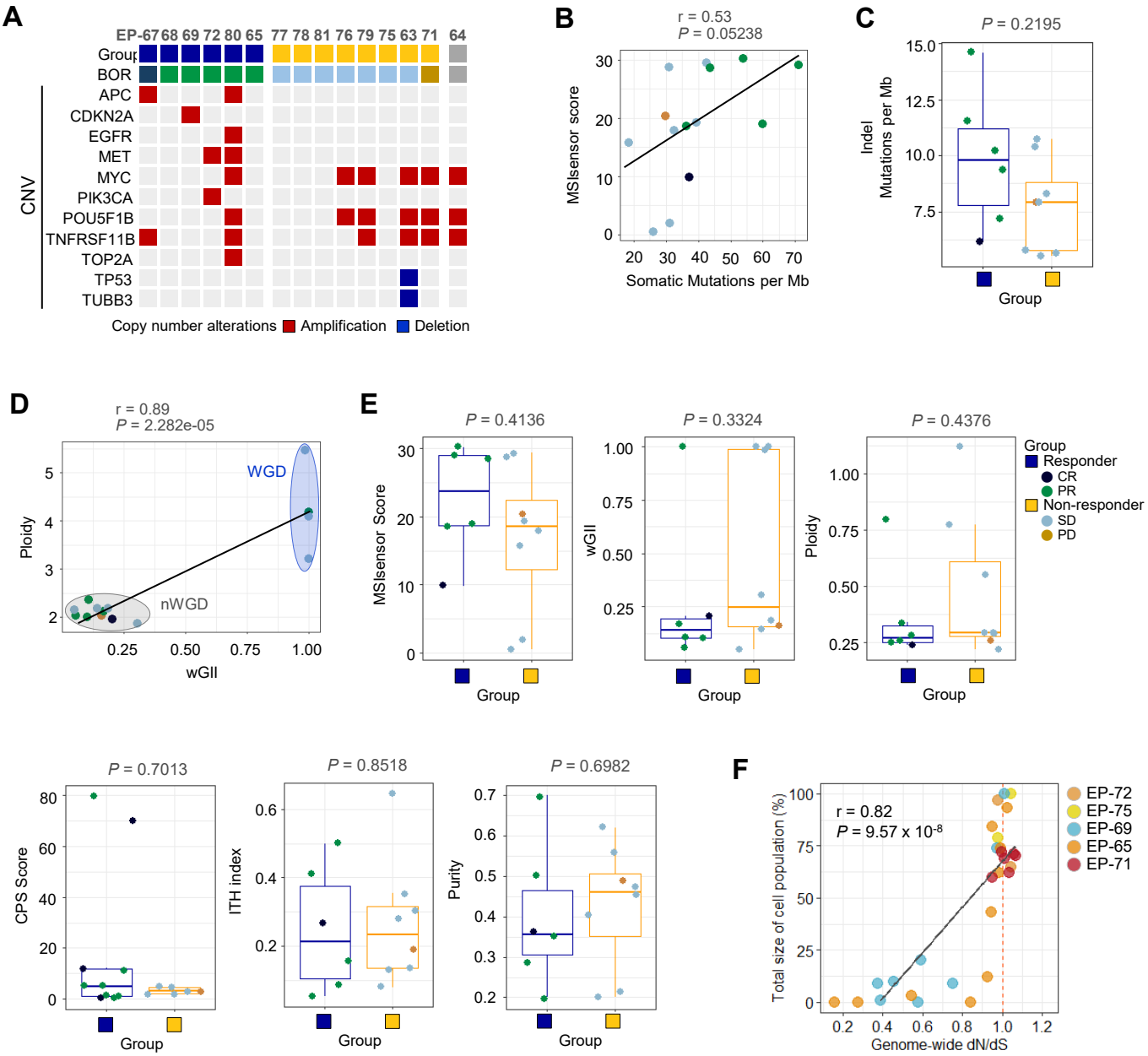

Supplemental figure S2. Genomic features of MSI-H GC

A. Landscape of copy number alterations in pre-pembrolizumab samples from the patients with MSI-H GC matched with the clinical response. **B.** Strong correlation between mutations per megabase (Mut/Mb) (TMB) and MSIsensor scores. **C.** Comparison of indel mutations per megabase (Mb) between responders and non-responders (Wilcoxon signed-rank test). **D.** Evaluation of the association between ploidy and genome instability (wGII: weighted genomic instability index). Ellipses correspond to the 95% probability region of each group. nWGD: non-whole-genome doubling, WGD: whole-genome doubling. **E.** Comparison of multiple genomic features between responder and non-responder groups. Statistical significance between two metrics was measured using a Wilcoxon signed-rank test. Boxplots represent the median, bottom, and top quartiles with whiskers extending to the maximum or minimum value. Colors of each dot indicate the group of best of response (BOR). **B** and **D.** Statistical significance between two metrics was measured using Pearson's correlation test. **F.** Correlation of dN/dS as a function of selective pressure in cancer evolution with the total size of the cell population across multiple biopsied samples. Pearson's correlation test was used to determine statistical significance. The dashed orange line indicates dN/dS = 1.

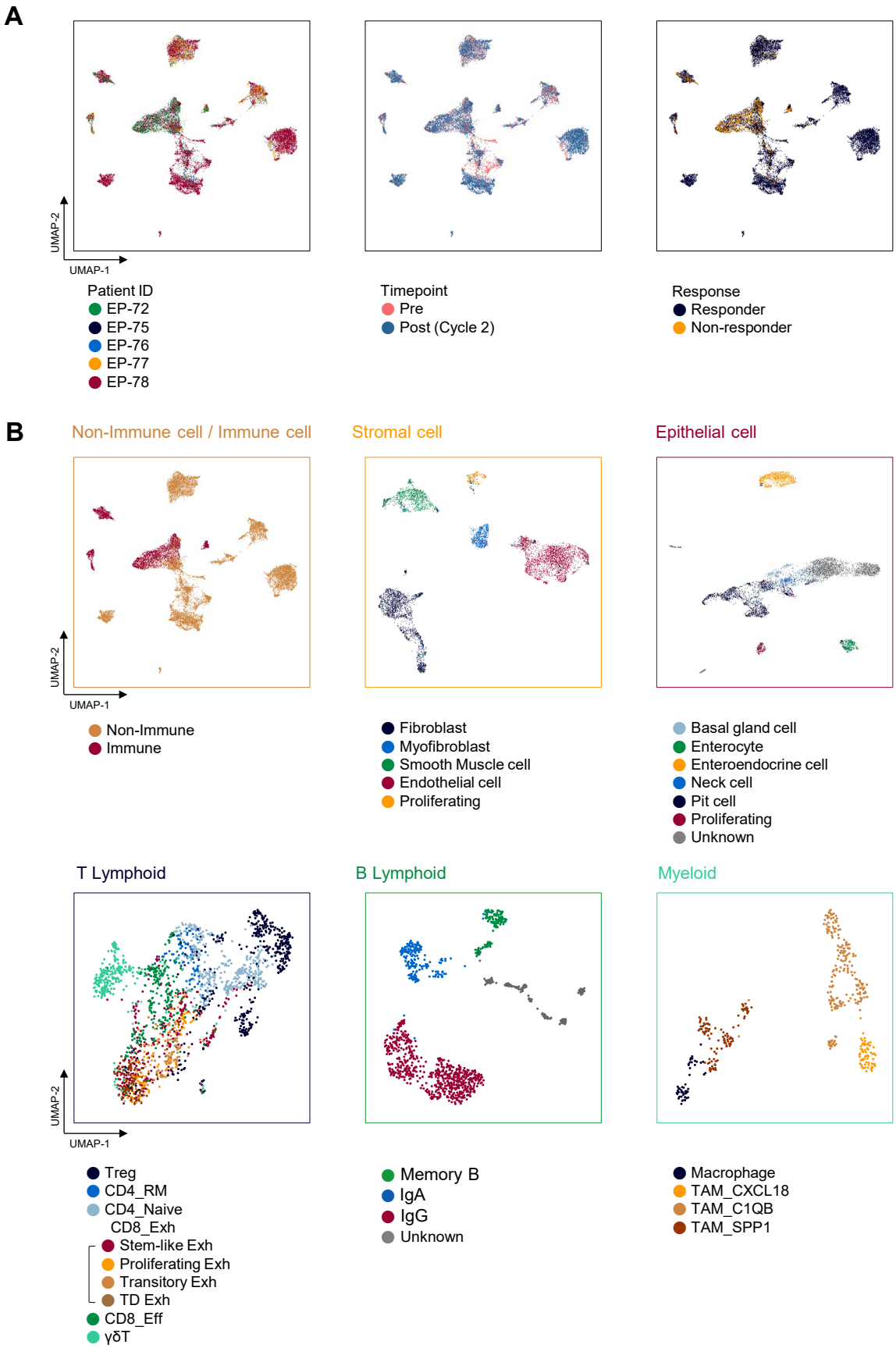

Supplemental figure S3. Single cell transcriptome map of MSI-H GC

A. Assessment of batch correction across patients, time points, and responses across total single cells. **B.** Identification of subtypes of non-immune/immune, stromal, epithelial, T lymphoid, B lymphoid, and myeloid cells colored according to assigned subpopulations.

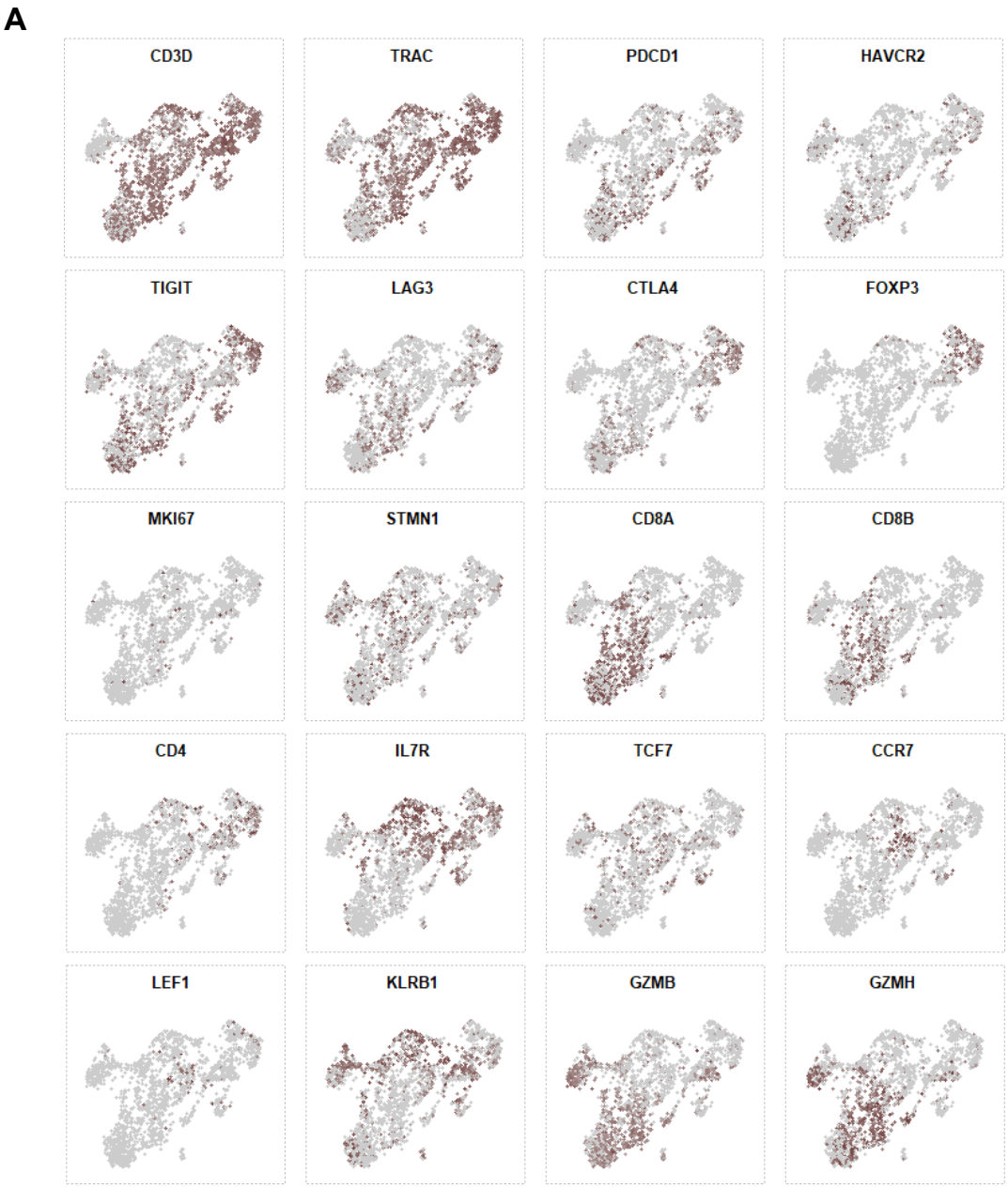

Supplemental figure S4. Gene markers for annotating T cells

A. UMAP of T cell subpopulation showing representative T cell markers. **B.** Heatmap of representative markers used in annotating exhausted T cell.

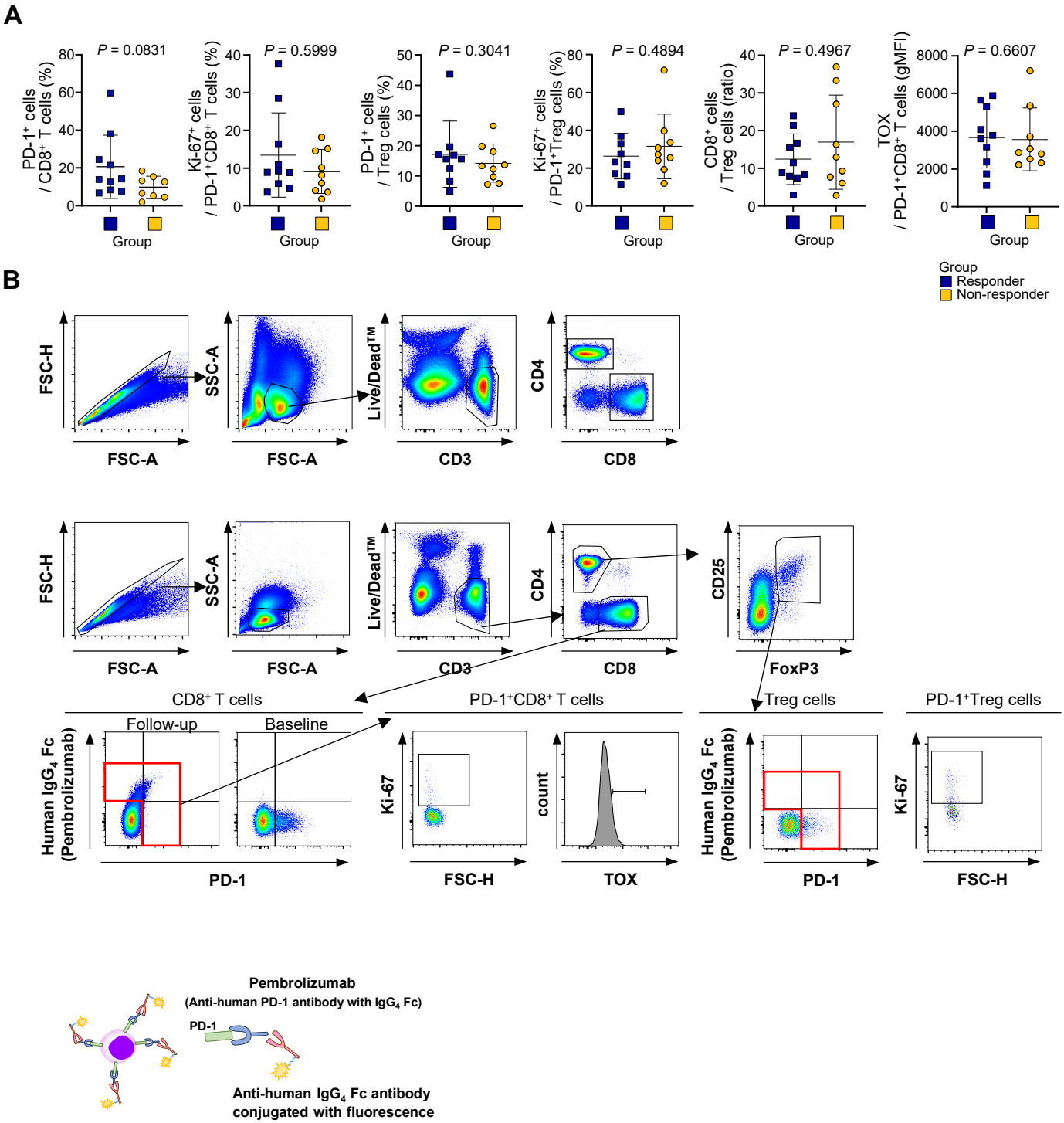

Supplemental figure S5. Association between immunophenotype of peripheral blood (PB) T cells and pembrolizumab response

A. The relative frequency of PD-1$^+$ cells among CD8$^+$ T cells, and Ki-67$^+$ cells among PD-1$^+$CD8$^+$ T cells and PD-1$^+$ regulatory T cells (CD3$^+$CD4$^+$CD25$^+$FoxP3$^+$), the relative frequency of PD-1$^+$ cells among regulatory T cells, the ratio of CD8$^+$ T cells to regulatory T cells, and the geometric mean fluorescence intensity of PD-1$^+$CD8$^+$ T cells in pre-pembrolizumab PB were compared between responders and non-responders (n = 19). Statistical analysis was performed using the Mann-Whitney test. **B.** Gating strategy to identify CD8$^+$ T cells and regulatory T cells. In the post-pembrolizumab sample, PD-1$^+$ cells were defined as positive populations in anti-PD-1 gating or anti-human IgG_4 gating (red box).